Characterization of the Thermal Structure inside an Urban Canyon: Field Measurements and Validation of a Simple Model

LORENZO GIOVANNINI AND DINO ZARDI

Atmospheric Physics Group, Department of Civil, Environmental and Mechanical Engineering, University of Trento, Trento, and National Consortium of Universities for Atmospheric and Hydrospheric Physics (CINFAI), Camerino, Italy

MASSIMILIANO DE FRANCESCHI

Atmospheric Physics Group, Department of Civil, Environmental and Mechanical Engineering, University of Trento, Trento, Major Seminary, Diocese of Bolzano-Bressanone, Bressanone, and National Consortium of Universities for Atmospheric and Hydrospheric Physics (CINFAI), Camerino, Italy

(Manuscript received 28 December 2011, in final form 24 July 2012)

ABSTRACT

The results of measurement campaigns are analyzed to investigate the thermal structure in an urban canyon and to validate a simplified model simulating the air and surface temperatures from surface energy budgets. Starting from measurements at roof-top level, the model provides time series of air and surface temperatures, as well as surface fluxes. Two campaigns were carried out in summer 2007 and in winter 2008/09 in a street of the city of Trento (Italy). Temperature sensors were placed at various levels near the walls flanking the canyon and on a traffic light in the street center. Furthermore, the atmosphere above the mean roof-top level was monitored by a weather station on top of a tower located nearby. Air temperatures near the walls, being strongly influenced by direct solar radiation, display considerable contrasts between the opposite sides of the canyon. On the other hand, when solar radiation is weak or absent, the temperature field remains mostly homogeneous. Moreover, air temperature inside the canyon is generally higher than above roof level, with larger differences during summertime. Air temperatures from the above street measurements are well simulated by the model in both seasons. Furthermore, the modeled surface temperatures are tested against a dataset of wall surface temperatures from the Advanced Tools for Rational Energy Use Towards Sustainability–Photocatalytic Innovative Coverings Applications for Depollution (ATREUS–PICADA) experiment, and a very good agreement is found. Results suggest that the model is a reliable and convenient tool for simplified assessment of climatic conditions occurring in urban canyons under various weather situations.

1. Introduction

The assessment of the microclimate inside an urban canopy—that is, in the atmospheric layer between the ground and the roof level (Oke 1976)—is relevant for many practical applications in different fields. Indeed, the thermal and dynamical structure of the atmosphere in an urban canopy is a key factor controlling pollutant dispersion and heat exchange between buildings and the surrounding environment. So the understanding of processes inside the urban canopy is a crucial prerequisite for the adoption of measures aiming at improving human comfort, protecting citizens' health, and supporting energy-efficient building design.

Several field measurements have been performed in the last few years to assess the temperature distribution inside urban canyons (cf. Grimmond 2006 for a review). The results of these campaigns partly reflect site-specific characteristics, but some features common to a variety of similar cases can also be highlighted. In particular, during daytime two opposite situations may occur, depending on the combination of the street aspect ratio (i.e., the ratio between the height of the buildings and the width of the street) and the solar zenith angle. Direct solar radiation can penetrate more inside the street when one of the above factors, or both, are low. This enhances the heat absorbed by sidewalls and road surface, so the air in the urban canyon becomes generally

Corresponding author address: Lorenzo Giovannini, Atmospheric Physics Group, Department of Civil, Environmental and Mechanical Engineering, University of Trento, Via Mesiano, 77, I-38123 Trento, Italy.
E-mail: lorenzo.giovannini@ing.unitn.it

DOI: 10.1175/JAMC-D-12-06.1

warmer than above roof level (Kanda et al. 2005). On the other hand, when aspect ratio and/or solar zenith angle are high, less solar radiation can penetrate inside the urban canopy, so air temperature inside the street may be lower than above roof level, as found in a deep canyon (aspect ratio of 3.3) in Athens by Georgakis and Santamouris (2006). Similar results were found by Bourbia and Awbi (2004) from measurements in the town of El Oued (Algeria): in the old part of the city (a traditional dense network of narrow alleys) the average temperature is lower than at a reference station outside the city center, whereas in the modern part (wide roads, large open spaces) the average temperature is higher.

During nighttime the aspect ratio generally plays an opposite role. In fact, a high aspect ratio, and thus a low sky view factor, reduces radiative cooling from an urban canyon, resulting in higher temperatures than in streets with lower aspect ratios (Svensson 2004). Indeed, a smaller sky view factor is one of the main causes of the nocturnal canopy-layer urban heat island (Oke 1981).

Urban canyons can also modify surface exchanges with the atmosphere on a larger scale and thus affect a range of phenomena. For this reason, to keep pace with the increasingly higher resolution attained by numerical weather prediction models, specific schemes have been developed to parameterize surface exchanges inside urban canyons, and between urban canyons and the atmosphere (cf. Masson 2006; Grimmond et al. 2008). In fact an urban canyon is commonly considered the fundamental unit of urban areas. Accordingly in mesoscale models surface fluxes are calculated as they arise from a single urban canyon with the average characteristics of the local urban morphology (Masson 2006; Chen et al. 2011). Indeed, more accurate parameterizations of urban effects, including urban canopy processes, are expected to improve the numerical simulation of wind structure, turbulence and diffusion, convection, and precipitation, even in connection with concurrent factors, such as land use heterogeneity and complex orography (Bertò et al. 2004; Shepherd 2005).

Several studies evaluated the performance of such urban-canyon models against measures of fluxes and surface temperatures (e.g., Masson et al. 2002; Pigeon et al. 2008). In particular an urban energy balance model comparison was recently performed to evaluate the ability of 32 different models to simulate surface fluxes (Grimmond et al. 2008, 2010, 2011).

However, concentrating mostly on energy fluxes and on the input parameters for meteorological models, less attention was paid to test the ability of such urban-canyon models to reproduce air temperature inside a specific street, as well as to a direct comparison with concurrent temperature measurements. Yet these simple models typically offer the advantage to require much shorter time than computational fluid dynamics models. Nevertheless, they can be reliably used to assess the main climatic conditions inside urban canyons. To the authors' knowledge, comparisons between the results of such models and air temperature measurements inside a specific urban canyon are still few in the literature. Lemonsu and Masson (2002) evaluated the performance of the town energy budget (TEB) model (Masson 2000) with measurements from a dense station network during summertime in Paris. Lemonsu et al. (2004) compared the output of the TEB model with measurements in Marseille during the Expérience sur Site pour Contraindre les Modèles de Pollution atmosphérique et de Transport d'Emissions (ESCOMPTE) campaign (Mestayer et al. 2005). Hamdi and Masson (2008) evaluated the multilayer version of TEB against measurements from the Basel Urban Boundary Layer Experiment (BUBBLE) field campaign in Basel (Rotach et al. 2005). The BUBBLE dataset was also used by Roulet et al. (2005) to test the multilayer building effect parameterization (BEP) model (Martilli et al. 2002). Finally, a slightly modified version of the BEP model was evaluated by Hamdi and Schayes (2007) against measurements in Basel and Marseille.

In the present paper a simple model is introduced that calculates the average air temperature inside an urban canyon from energy budgets on the different surfaces inside the street. This model shares many concepts adopted in the above urban parameterizations and in particular in the single-layer model by Kusaka et al. (2001). This model complements the results from two measurement campaigns, carried out in the summer 2007 and in the winter 2008/09, as part of a project aimed at evaluating microclimatic conditions in an urban canyon in the city of Trento (Italy). The above campaigns provided a dataset of air temperatures close to the walls and in the street center, which allowed us to test how the model performs in reproducing the average air temperature within the canyon. Unfortunately no surface temperature measurements could be taken during the field campaigns in Trento. Therefore a supplementary dataset of wall surface temperature from the Advanced Tools for Rational Energy Use towards Sustainability–Photo-catalytic Innovative Coverings Applications for Depollution (ATREUS–PICADA) experiment (Idczak et al. 2007) was adopted to further test the model results.

Accordingly, the paper is organized as follows. The two field campaigns in Trento are presented in section 2, where data from temperature measurements inside the urban canyon are analyzed and compared with the environmental conditions measured above roof level. In section 3 the main model features and setup are described, while in section 4 the model is validated against measurements from the ATREUS–PICADA experiment and observations taken

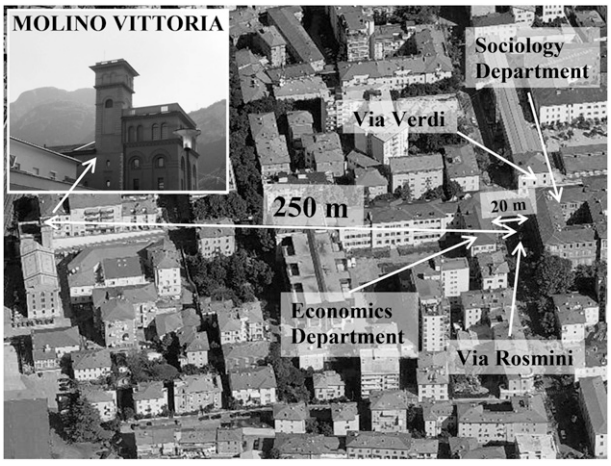

FIG. 1. Aerial photo showing the street canyon adopted as test case, Via Rosmini, and Molino Vittoria weather station. The double-headed arrow on Via Rosmini indicates the cross section where instruments were placed during the field campaigns. (Photograph is provided through the courtesy of the Municipality of Trento).

in Trento. Considerations about the surface fluxes simulated by the model are also presented in this section. In section 5 results are summarized and commented, while in section 6 some conclusions are drawn along with an outlook for future developments. The modifications introduced in the model with respect to the original scheme of Kusaka et al. (2001) are summarized in the appendix.

2. Field measurements

a. Site description and instrumental setup

Two fields measurements were carried out, respectively from 26 July to 20 August 2007 and from 23 December 2008 to 22 January 2009, in a street canyon of the city of Trento. The latter is a midsized city of 56 000 inhabitants (Municipality of Trento 2009), lying in the Adige Valley, in the southern side of the Alps, at 200 m MSL. In a previous work (Giovannini et al. 2011), the urban heat island of the city was evaluated comparing temperature measurements taken within the city center and at surrounding rural locations.

The purpose of the present campaigns was to investigate the thermal field inside the urban canopy in different seasons, to highlight the effects of the different penetration of solar radiation. Measurements were carried out in the urban canyon of Via Rosmini, close to the historic city center of Trento, in the middle of the whole urban area (Fig. 1). The core of the city center is built over the old Roman city and displays the typical regular grid of streets crossing at right angles. Accordingly it presents a compact morphology with high values of the building plan area fraction $\lambda_p = A_p/A_t$, where A_p is the plan area of buildings and A_t is the total area, and of the frontal area index $\lambda_f = A_f/A_t$, where A_f is the area of the walls perpendicular to the wind (Grimmond and Oke 1999). The former ranges between 0.5 and 0.8, while the latter between 0.25 and 0.35, for both northerly and southerly winds, which are the dominant directions, following the north–south-oriented valley (Giovannini et al. 2011). The above values were calculated by means of GIS techniques, based on the high-resolution (1 m) dataset from airborne lidar scans provided by the Municipality of Trento. In the city center building heights are rather homogeneous, excluding few medieval towers, ranging from 15 to 20 m, and the vegetation fraction is very low (<5%–10%).

The selected street offers a suitable test case, with a very simple geometry: buildings of equal heights flank the street, and vegetation is limited to low, sparse deciduous trees on the sidewalks. It is one of the main streets of the city, running straight for about 350 m in both directions from the measurement points (Fig. 1). The building walls facing the street are constructed with brick and concrete, and covered with plaster, while the street ground is asphalted. Via Rosmini is roughly north–south oriented (354°N) and displays an average width $w \approx 20$ m, while the buildings at both sides display a rather uniform height $h \approx 17$ m. This implies an average aspect ratio $h/w \approx 0.85$.

Five Onset, Inc., Model HOBO H8 Pro devices were used for the measurements. These instruments are composed of a temperature and humidity sensor covered by a solar-radiation screen, with eight superimposed plates. These low-cost instruments display good characteristics of accuracy (0.2°C declared by the manufacturer) and have been widely used, under various setups, for meteorological research, also in the urban environment (Whiteman et al. 2000; Doran et al. 2003; Fast et al. 2005). They include a memory unit and a long-term battery, which allowed them to operate in a stand-alone mode for the entire periods of the campaigns.

Before the field measurements the sensors were intercompared in a controlled ambient room, and the resulting data were all within the accuracy range provided by the manufacturer. The sensors were setup to take measurements every 5 min in the so-called high-resolution mode (12 bit).

The instrumental setup is shown in Fig. 2. In both campaigns four sensors were placed on the two opposite walls of Via Rosmini (belonging to the Sociology and Economics Departments, respectively), two per wall at a height of about 7 and 11 m AGL, respectively. In the winter campaign an additional HOBO was installed on a traffic light in the center of the street at 7 m AGL to evaluate also the temperature inside the street not directly

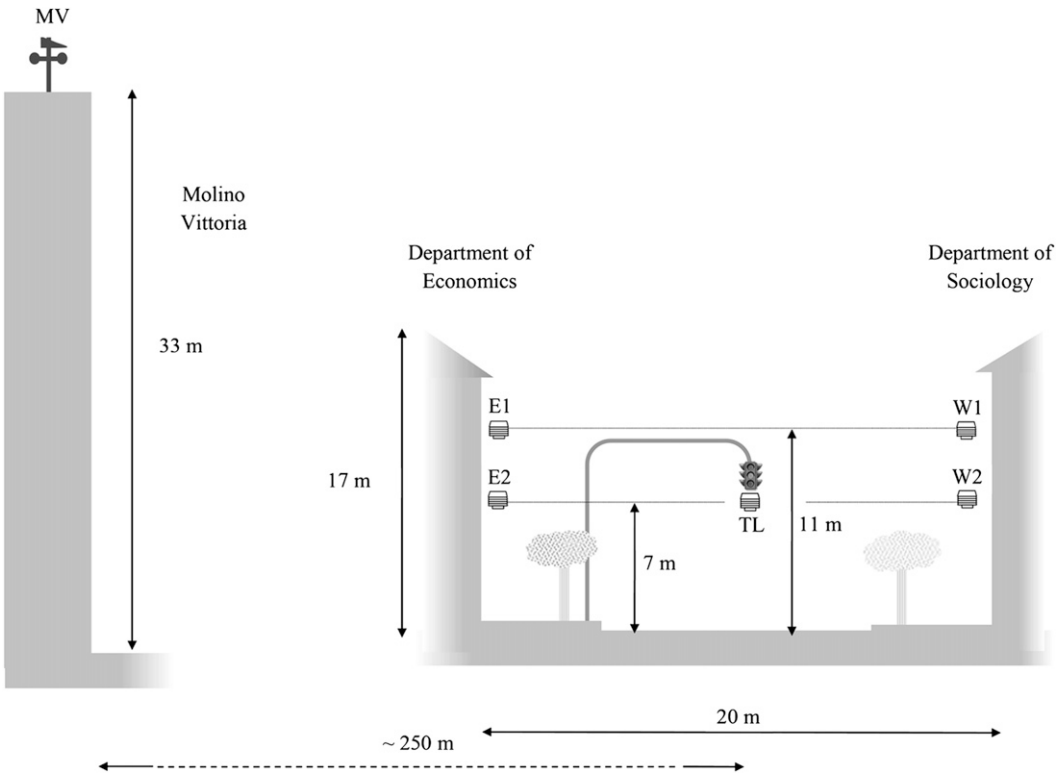

FIG. 2. Schematic representation of the cross section analyzed along with the positions of the HOBOs inside the street.

influenced by any surface (Fig. 3). For convenience the sensors on the walls are identified with a label indicating the direction they were facing (E = east, W = west), and the level they were placed (1 = higher, 2 = lower): for example, E1 means the east-facing higher sensor at 11 m AGL. The sensor on the traffic light is labeled TL.

The measuring section lies in a stretch of street with a length $L \approx 50$ m between two subsequent intersections. This implies a ratio $L/w \approx 2.5$. The horizontal distance of the sensors from the closest (northern) corner of the buildings, corresponding to the intersection with the west–east-oriented Via Verdi (Fig. 1), is about 10 m. To test the possible influence of the intersection on the measurements, an additional HOBO was installed at 11 m AGL on the north-facing façade of the Sociology Department in Via Verdi during the summer field campaign. Results showed no significant temperature contrasts with the sensors in via Rosmini. The only differences were caused by the different exposure to direct solar radiation, similarly to the results found in Via Rosmini [see sections 2d(1) and 2d(2)].

For temperature measurements near canyon walls, it is important to evaluate the influence of the thermal boundary layer developing on a sunlit wall. Idczak et al. (2007) found a thermal boundary layer of about 50 mm, and the thickness was rather independent from temperature. Farther from the wall the air temperature remained higher than in the center of the canyon, but the horizontal temperature gradient became considerably lower.

Accordingly the sensors in the two measurement campaigns in Trento were installed at about 0.3 m from the walls to evaluate the effects of the surface heating on the air temperature near the walls, yet outside the thermal boundary layer. A similar setup was adopted by Santamouris et al. (1999) in Athens and by Erell and Williamson (2007) in Adelaide (Australia).

Via Rosmini is approximately 250 m far away from the automated meteorological station of Molino Vittoria (Fig. 1), permanently operated by the Atmospheric Physics Group of the University of Trento (Giovannini et al. 2011; Grigiante et al. 2011). The station is based on top of a tower at 33 m AGL, that is, roughly twice the height of the surrounding buildings. Given the site characteristics, these measurements are taken at the lower boundary of the inertial sublayer, where the single microclimatic anomalies are mixed. So the station sensors probe a blended, spatially averaged signal, representative of the local scale (Oke 2006). For this reason, measurements taken at this station, and recorded as 10-min averages, were assumed as representative of weather

FIG. 3. Positions of the five HOBOs used during the field measurements.

conditions above the average roof-top level and adopted for comparison with data taken inside the canyon.

b. Direct solar radiation

The penetration of direct solar radiation inside the street is a key factor for temperature distribution in the canopy layer. The sky lines viewed at ground level from the two walls flanking Via Rosmini and the path of the sun in the sky during the periods of the two field campaigns are shown in Fig. 4. The higher arch corresponds to the summer field measurements (upper curve: 26 July, lower curve: 20 August), whereas the lower arch corresponds to the winter field measurements (upper curve: 22 January, lower curve: 23 December). Notice that the two walls are lit by direct solar radiation over different periods in the two campaigns: in summertime the east-facing wall (Fig. 4a) gets direct solar radiation at ground level approximately from 0800 to 1200 LST (UTC + 1), whereas the west-facing wall (Fig. 4b) from 1200 to 1630 LST. In winter these periods are considerably shorter: at ground level the east-facing wall is lit from 1030 to 1200 LST, while the west-facing wall is lit from 1200 to 1430 LST. Obviously, the higher portions of the walls get direct solar radiation for longer than the lower ones: indeed, sunrise time at the top of the east-facing wall is as early as 0600 LST during the summertime and at 0930 LST in winter, while sunset time at the top of the west-facing wall is delayed at 1815 LST in summertime and at 1500 LST during the wintertime.

c. Weather conditions

Weather conditions during the field measurements are well documented by hourly cloud-cover observations (in oktas) taken at the weather station on top of Mount Paganella. The latter is operated by the Italian Air Force Weather Service, at 2125 m MSL on the western side of the Adige Valley, 10 km northwest of Trento. Days were grouped into three weather categories, based on the average daily cloud cover: sunny days (0–2 oktas), partly cloudy days (2–6 oktas), and cloudy or rainy days (6–8 oktas). In the summer campaign 11 sunny days, 12 partly cloudy days, and 3 cloudy or rainy days were registered. Air temperature measured at Molino Vittoria ranged from 14.0° to 33.6°C. In the winter campaign there were 17 sunny days, 9 partly cloudy days, and 4 cloudy or rainy–snowy days and air temperature at Molino Vittoria ranged from −6.2° to 11.6°C. Temperature measurements at Molino Vittoria and cloud-cover observations at Mount Paganella during both the summer and the winter field campaigns are shown in Figs. 5 and 6, respectively.

The analysis presented in the next sections concentrates especially on three representative days: one for the summer campaign (5 August, a sunny day), and two for the winter (11 January, a sunny day, and 6 January, a rainy–snowy day). The analysis of temperatures in these days allows us to highlight the recurrent behaviors observed during the two field campaigns under different weather conditions. The graphics in Fig. 7 show relative humidity, wind speed, and direction measured at Molino Vittoria in these three days, to further characterize the weather conditions occurred.

d. Data analysis

1) SUMMER FIELD MEASUREMENTS

During the summer measurements the four HOBOs worked correctly for all the period, and all the data

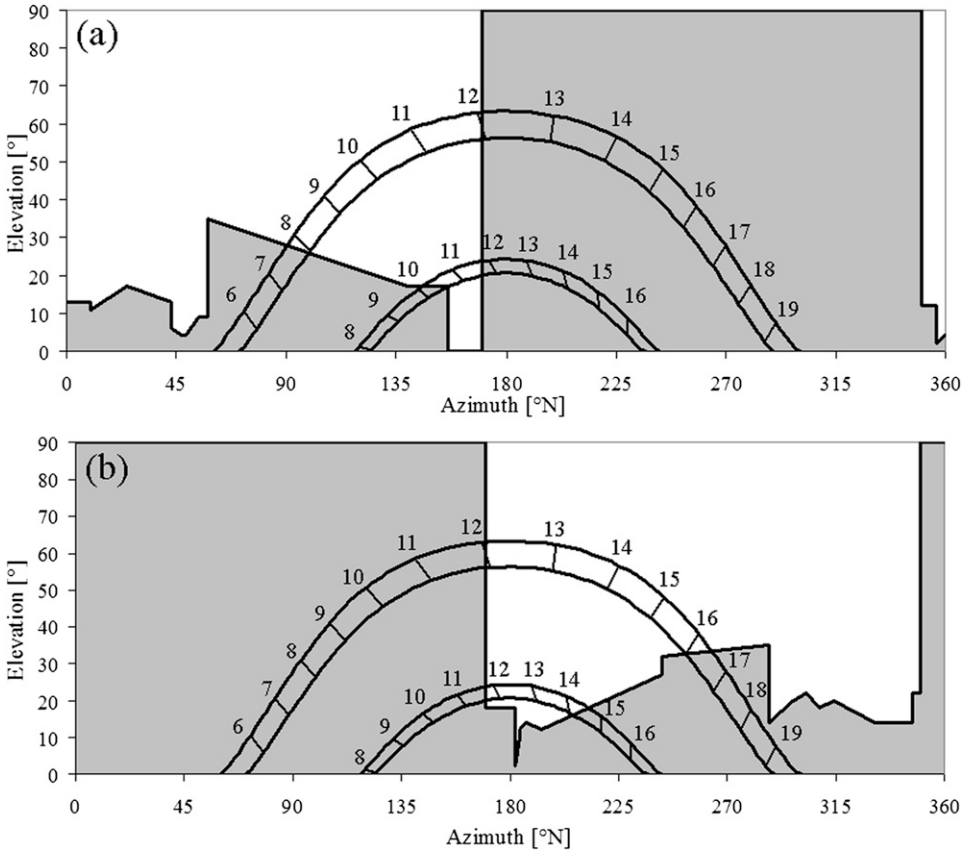

FIG. 4. Sky lines as viewed at ground level from (a) the east-facing and (b) the west-facing walls of Via Rosmini. In both panels the diurnal path of the sun in the sky and the relative hourly position are shown. The higher arch corresponds to the period of the summer field campaign (lower curve 20 Aug and upper curve 26 Jul), whereas the lower arch corresponds to the period of the winter field campaign (lower curve 23 Dec and upper curve 22 Jan).

registered could be used in the data analysis. The measurements taken inside the canyon and at Molino Vittoria in the reference sunny day are shown in Fig. 8. For the sake of clarity data have been downsampled to 30-min averages: this representation on one side still allows us to capture the relevant timing of changes in the temperatures inside the canyon, on the other side is consistent with the representation of Idczak et al. (2007) for the ATREUS–PICADA experiments.

In the morning the east-facing sensors warm up faster than the other ones, while in the afternoon the west-facing instruments are the warmest. In the morning the temperature measured by the sensors on the sunlit wall is around 2°C higher than the sensors in the shade, while in the afternoon the temperature difference is slightly lower, 1.5°C on average. The difference is probably bigger in the morning because the east-facing wall, which was heated in the morning, releases energy in the afternoon, inducing a reduction of the temperature difference between the opposing sensors (Hamdi and Schayes 2008). Moreover, in the afternoon, even during sunny days, cumulus clouds sometimes covered the sun, thus lowering the heating of the west-facing wall.

Focusing on the differences between the sensors on the same wall, during daytime, and especially when both HOBOs are hit by direct solar radiation, the lower instrument systematically records a temperature slightly higher (about 0.5°C). This is probably to be attributed to the warming from road asphalt.

At night temperature values are generally similar for all the four instruments, with differences mostly below 0.5°C. However, slightly higher temperatures are generally measured by the east-facing sensors, especially in the evening, probably because the east-facing wall absorbs more solar radiation in the morning.

Temperature differences between the four HOBOs during partly cloudy days follow the same behavior as during sunny days, but with smaller differences, because of the lower solar forcing. On the other hand in cloudy or rainy situations, when solar radiation is

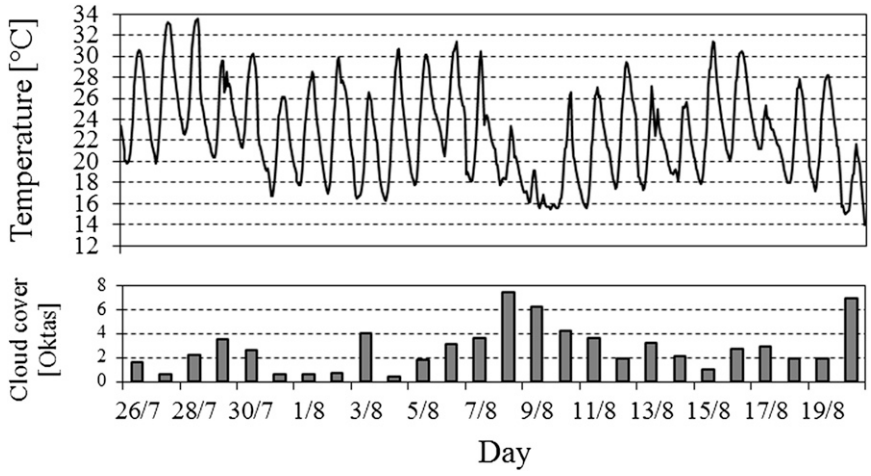

FIG. 5. (top) Air temperature (hourly averages) measured at Molino Vittoria and (bottom) cloud cover (daily averages) observed at Mount Paganella weather station during the summer field measurements.

very low, differences between the four HOBOs are negligible.

Comparison with measurements above roof level from Molino Vittoria shows that the HOBOs record temperatures systematically higher, under every weather condition. In clear-sky situations, during nighttime the temperature inside the canyon is about 1°C higher than above roof level for all the four HOBOs, while during daytime the temperature differences between the sensors inside the canyon and Molino Vittoria vary in connection with direct solar radiation (Fig. 8). The sunlit sensors are on average 2°–2.5°C warmer than at Molino Vittoria. However, differences as high as 3°–3.5°C are recorded in some days, especially when the sky is completely clear and thus solar radiation is stronger. In the morning the temperature of the sensors in shade is about the same as measured at Molino Vittoria. On the other hand during the afternoon, even the sensors in shade register temperatures higher than Molino Vittoria. These differences change day by day, yet displaying an overall average difference of order 1°C. This behavior may be attributed to the heat released by the east-facing wall, as mentioned above.

Finally the temperature measured by the four instruments in the canyon is constantly higher than recorded at Molino Vittoria even during cloudy or rainy days, with average differences of order 1°C.

2) WINTER FIELD MEASUREMENTS

The winter field measurements were affected by some technical problems with the west-facing sensors, so after a quality check some data recorded by these HOBOs were discarded. In particular 7 and 19 days of data registered respectively by W1 and W2 were used for the

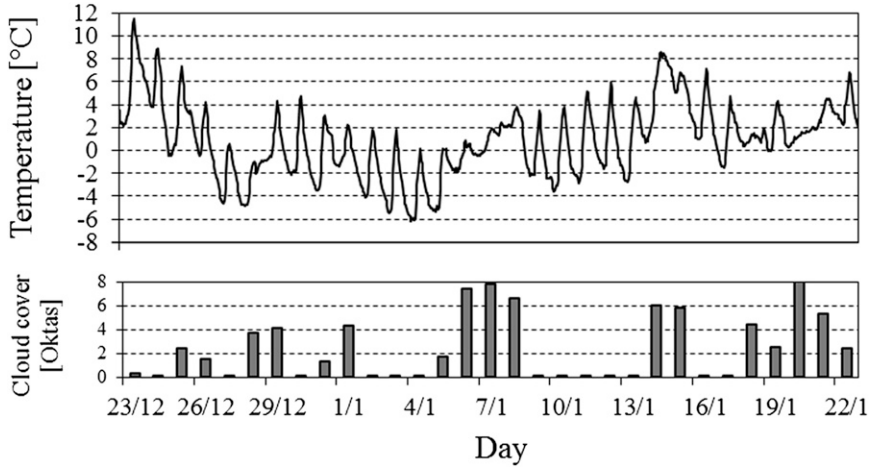

FIG. 6. As in Fig. 5, but for the winter field measurements.

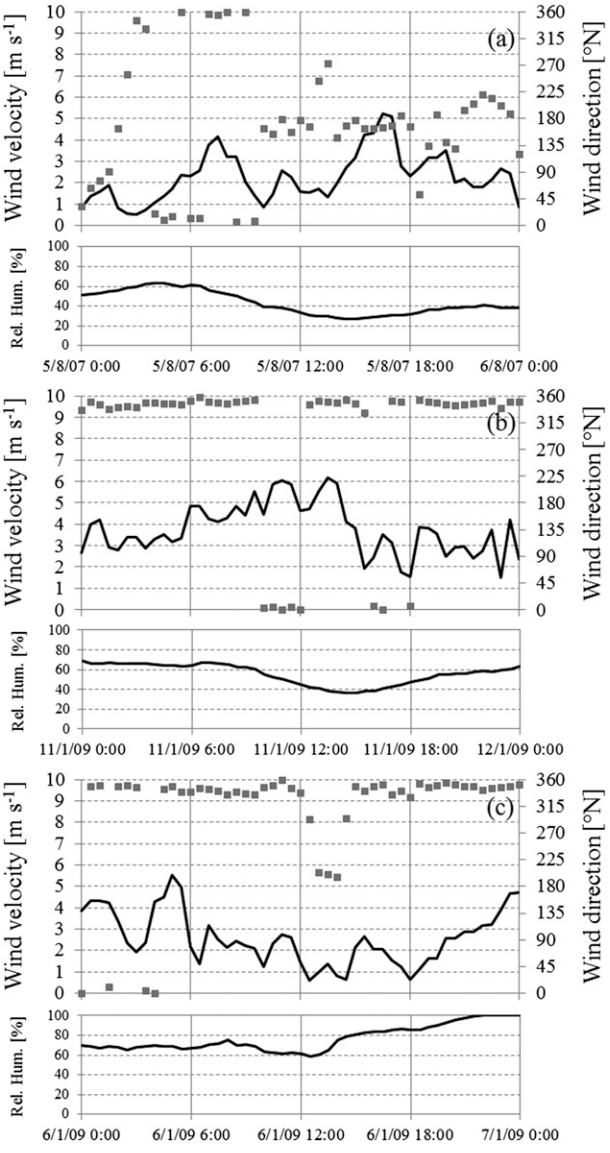

FIG. 7. Relative humidity, wind speed, and direction measured at Molino Vittoria weather station in (top to bottom) the three days taken as a reference to analyze the data of the field measurements.

present analysis. The other sensors performed correctly for all the 31 days of the field measurements. The daily cycle for all the available sensors (30-min averages) for the reference sunny day is shown in Fig. 9. Temperatures near canyon sidewalls are still influenced by direct solar radiation, but with some remarkable differences from summer measurements. In particular the overheating of the east-facing sensors in the morning is almost negligible, as solar radiation is very weak during these hours and hits this wall for a shorter time (Fig. 4a). On the contrary during the afternoon the overheating of the west-facing sensors is considerable (2°C on average). The maximum temperature measured by the west-facing

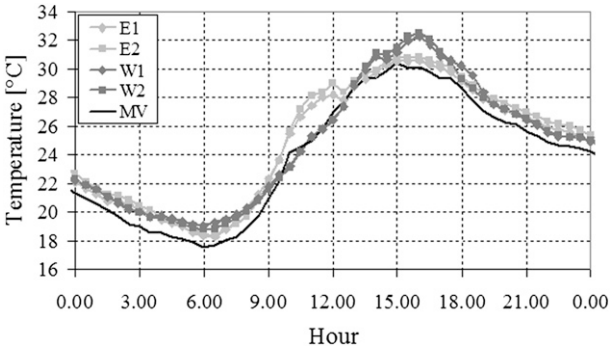

FIG. 8. Comparison of air temperature measurements taken inside the urban canyon and at Molino Vittoria. The values presented here are 30-min averaged temperatures for 5 Aug 2007, a sunny day. Each curve refers to one sensor, identified with a label: E, W indicate sensors facing respectively east and west; 1 and 2 indicate higher and lower heights, respectively. MV indicates measurements taken over roof level at Molino Vittoria.

sensors occurs at 1500 LST, an hour earlier than in summer, because of the earlier sunset time. The temperature measured by TL, which is not influenced by any surface, is always close to that registered by the sensors in shade during the whole diurnal cycle. At night and in cloudy or rainy–snowy days the five HOBOs display, as in the summer period, similar temperatures, with differences below the sensors accuracy, as can be seen in Fig. 10, where the diurnal cycle for the rainy–snowy day adopted as a reference is shown.

Comparison with measurements taken at Molino Vittoria shows that also during the winter period the temperature inside the urban canyon is generally higher than above roof level, although differences are lower than during the summer field measurements. At night and during cloudy or rainy–snowy days the temperature inside the canyon is slightly higher (on average about 0.5°C) than above roof level. During daytime on sunny days (Fig. 9) the morning temperature above roof level is similar to that measured by all sensors because of the above mentioned low overheating of E1 and E2. However, in the afternoon the HOBOs facing west are on average 2°C warmer than Molino Vittoria, while the east-facing sensors and TL measure a temperature similar to Molino Vittoria. In some cases in the afternoon the temperature at Molino Vittoria is even higher than registered inside the canyon by the sensors in the shade.

3. Model description and setup

a. Model description

The simple two-dimensional model implemented here and validated against field measurements is a slightly modified version of the single-layer model by Kusaka

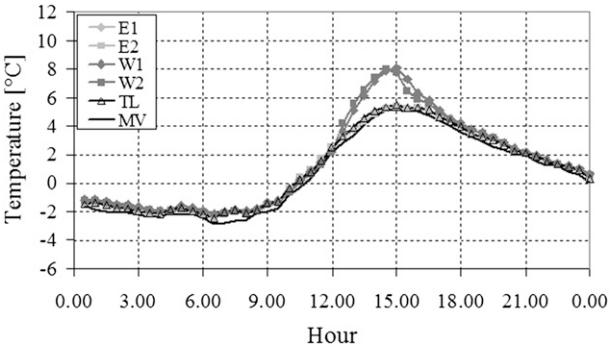

FIG. 9. As in Fig. 8, but for 11 Jan 2009, a sunny day. The TL indicates data taken on a traffic light in Via Rosmini.

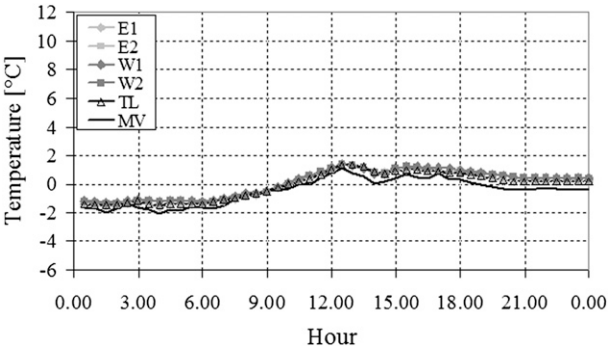

FIG. 10. As in Fig. 9, but for 6 Jan 2009, a rainy–snowy day.

et al. (2001). The main characteristics of the model are outlined in this section, whereas the few modifications from the original scheme of Kusaka et al. (2001) are shown in appendix A.

The numerical scheme can simulate the average air temperature in an urban canyon by calculating separate surface energy budgets for each surface (road, walls, and roof). The model balances the heat fluxes inside a suitable control volume, so that the heat exchanged through the top of the canyon (which is the interface between the canyon and the over-the-canopy atmosphere) equals the heat released–absorbed by the ''physical'' surfaces, that is, walls and road. Moreover, the model takes into account the shadowing inside the street and the multiple reflections of both short- and longwave radiations between the road and the walls. The heat flux through the surfaces is calculated from the heat conduction equation dividing each surface in several layers.

The model implemented here calculates a dry surface energy budget (i.e., latent heat flux is not accounted for). However, it can be safely assumed that in an urban environment with scarce vegetation, such as the present cases, latent heat flux is very low (Oke et al. 1999). On the other hand, the model takes directly into account the anthropogenic heat flux from vehicular traffic in the form of a daily cycle that is added to the heat balance of the canyon. Heat fluxes from domestic heating or cooling are implicitly considered setting a constant temperature inside the buildings. On the other hand, at the present stage, heat directly released from other anthropogenic activities, such as air conditioners, is neglected. Indeed, this factor may be relevant at an urban-canyon scale (Ohashi et al. 2007; de Munck et al. 2013), but it is not expected to be crucial for the case at hand, as heat exchangers are mostly on rooftops.

The upper boundary conditions needed by the model are the basic meteorological parameters normally provided by standard weather stations: air temperature, relative humidity, incoming global shortwave radiation, and wind speed measured above roof level. The other basic inputs needed by the model are the cloud cover, the geometrical parameters of the canyon, and surface material properties.

b. Model setup

1) ATREUS–PICADA SIMULATION

The ATREUS–PICADA experimental campaign was carried out from 7 July 2004 to 20 October 2004 to study the microclimatic conditions inside urban canyons (Idczak et al. 2007). Measurements were taken on a physical model at 1:5 scale composed of four rows of steel containers simulating buildings (18.3 m in length, 5.2 m in height, and 2.4 m in width). The orientation of the street was 54°N, while the street width was 2.1 m, resulting in an aspect ratio of 2.5. The walls of the canyon were lined with white cement panels. Intensive measurements of the relevant atmospheric parameters, as well as of surface temperatures, were taken inside and outside the canyons. Here the performance of the numerical model is tested against data from their measurements of wall surface temperature at different heights in a sunny day (Fig. 10 of Idczak et al. 2007). The forcing meteorological parameters are provided in Idczak et al. (2007), along with the geometric characteristics of the canyon. The composition of canyon surfaces are taken from Idczak et al. (2010), where the authors compared the observations of the experimental campaign with the results of numerical simulations with a 3D finite elements model. Values adopted for the simulation are summarized in Table 1.

The aerodynamic roughness length z_0 and the displacement height d, required by the numerical scheme, are difficult to estimate because of the particular configuration of the physical model and the nonuniform conditions around the site. On the other hand, some preliminary tests highlighted that wall temperatures simulated by the model are not so sensitive to these parameters.

TABLE 1. Physical properties of the materials composing the canyon surfaces in the physical model of the ATREUS–PICADA experiment. Here d_l is the thickness of each layer (m), α is the albedo, ε is the emissivity, λ is the thermal conductivity (W m^{-1} K^{-1}), and C is the heat capacity (J m^{-3} K^{-1}).

		d_l	α	ε	λ	C
Walls	Cement	0.013	0.60	0.95	0.90	1 600 000
	Air layer	0.030	—	—	0.026	1206
	Steel	0.003	—	—	45.3	3 915 000
Ground	Gravel	0.35	0.20	0.95	1.6	2 288 000
	Soil	2.0	—	—	1.0	2 160 000
Roof	Steel	0.003	0.20	0.95	45.3	3 915 000

Accordingly, for the purpose of the present paper, the values proposed by Grimmond and Oke (1999) in their Fig. 1a for isolated roughness elements were supplied, namely, $d/h = 0.1$ and $z_0/h = 0.04$.

2) SIMULATIONS IN THE REAL CANYON

The ability of the model to simulate the air temperature inside an urban canyon is tested against the measurements from the field campaigns in Via Rosmini. As the model calculates the average air temperature inside the canyon, numerical results are compared with the measurements reasonably representing an average air temperature in the canyon. It can be safely assumed that the latter is provided by the HOBO placed on the traffic light during the winter field campaign. As to the summer campaign (when no measurements were taken at the street center), the sensors show that the temperature field is rather homogeneous during the night inside the street. So the numerical results are compared with the average of the four sensors. On the other hand, during daytime the sunlit sensors are influenced by the wall surface heating, so the HOBOs in the shade only can be taken as representative of the average conditions inside the street. In fact, as seen above, in wintertime the sensors in the shade always record a similar temperature to that measured in the street center. For this reason during daytime the model results are compared with the average of the observations of the two sensors in the shade.

In these simulations the upper boundary conditions are supplied by Molino Vittoria weather station, while the canyon parameters are shaped on Via Rosmini. The displacement height d and the aerodynamic roughness length z_0 are assumed to be constant for all possible wind directions around the test site. In fact the urban morphology in the area surrounding the canyon is quite homogeneous. In particular the values of λ_p and λ_f (for northerly and southerly winds, the prevailing directions occurring in Trento) range from 0.5 to 0.6 and from 0.2 to 0.3, respectively, considering 300 m both in the south and in the north directions from the analyzed street section. Building heights range between 13 and 18 m. The values of the displacement height and of the aerodynamic roughness length used in the model are borrowed again from Grimmond and Oke's (1999) Fig. 1. The values of λ_p and λ_f in the area surrounding the canyon correspond to $d/h = 0.8$ and $z_0/h = 0.08$. In this case the height h is 17 m, that is, the mean height of the buildings flanking the canyon, which is also representative of the surroundings. Furthermore, consistently with these values of λ_p, the width of the buildings is 30 m. For what concerns the real composition of the canyon surfaces, materials and widths of the different layers are assigned considering the usual engineering practice in the region (Table 2). Walls are assumed to be made of concrete, with a thin layer of insulating material, while roofs are in tiles covering a thin layer of insulating material and an internal layer of concrete. The temperature inside buildings is set constant at 26°C during summertime and 21°C during wintertime, assumed as average working conditions. Finally, the road is assumed to be made of asphalt over a layer of gravel, and natural soil at deeper levels. Moreover, at 1.25 m underground a constant temperature of 20°C in summer and 10°C in winter is assigned. The anthropogenic heat flux from vehicular traffic is calculated from the hourly vehicular fluxes provided in the Urban Mobility Plan of the Municipality of Trento. The daily cycle presents two peaks, one in the morning and one in the evening, with maximum values of order 7–8 W m^{-2}.

TABLE 2. As in Table 1, but for Via Rosmini.

		d_l	α	ε	λ	C
Walls	Concrete	0.01	0.30	0.90	1.51	1 540 000
	Concrete	0.09	—	—	1.51	1 540 000
	Insulation	0.01	—	—	0.03	250 000
	Concrete	0.30	—	—	1.51	1 540 000
Ground	Asphalt	0.01	0.10	0.95	0.82	1 740 000
	Asphalt	0.04	—	—	0.82	1 740 000
	Gravel	0.2	—	—	2.1	2 000 000
	Soil	1.0	—	—	0.4	1 400 000
Roof	Tile	0.01	0.20	0.90	1.4	1 510 000
	Tile	0.04	—	—	1.4	1 510 000
	Insulation	0.01	—	—	0.03	250 000
	Concrete	0.20	—	—	1.51	1 540 000

4. Model validation

a. Wall temperatures

The comparison between the wall temperatures simulated by the model and measured during a sunny day of the ATREUS–PICADA experiment is shown in Figs. 11 and 12 for the south and north walls, respectively. The model reproduces reasonably well the principal features

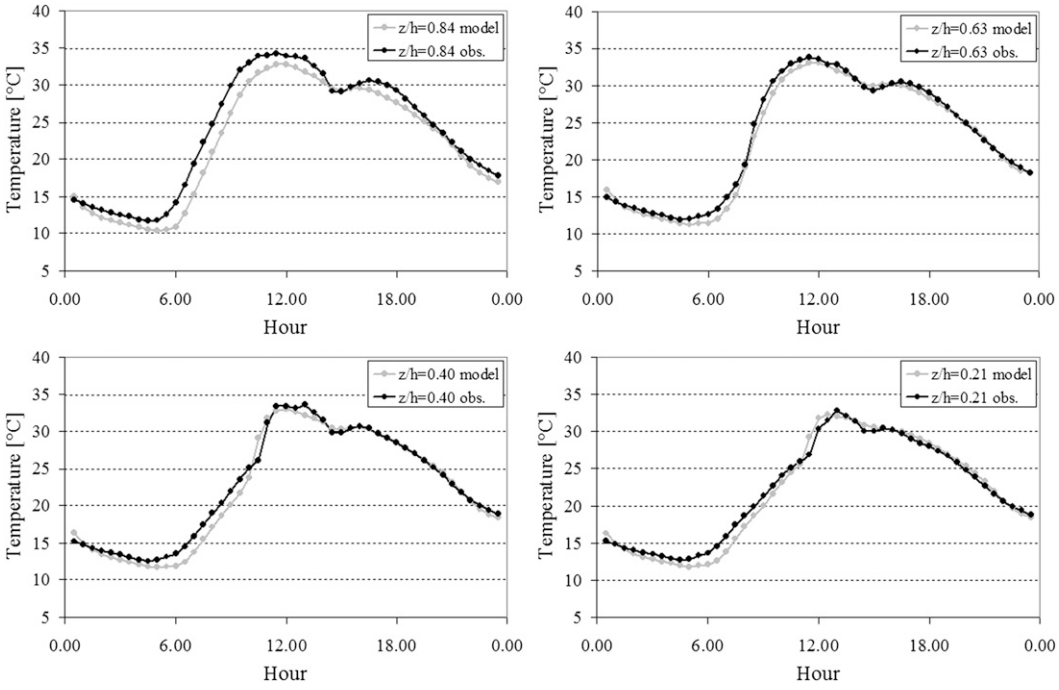

FIG. 11. Comparison (30-min averages) between the south wall temperatures measured at different heights during a sunny day of the ATREUS–PICADA experiment (black) and simulated by the model (gray).

of the daily cycles, including the primary peak, caused by direct solar radiation, and the secondary peak, which is due to reflections and emissions from the opposite wall. The mean absolute error of the model (MAE = $(1/n)\sum_{i=1}^{n}|f_i - y_i|$, where f_i is the model result and y_i the observation) is 0.9°C for the south wall and 1.2°C for the north wall. The highest errors are registered at the uppermost measurement points for both walls (MAE are 1.6° and 1.9°C for the south and north walls, respectively), where the model constantly underestimates the temperature. During nighttime these errors might be caused by an underestimate of the downward longwave radiation (minima are underestimated at all the measurement points). On the other hand, during daytime the heating of the steel roof of the container, a factor not taken into account by the model, might play a role.

When a wall is not lit by direct solar radiation, the model provides a wall temperature slightly decreasing with height from ground up to roof level. Indeed, the lower parts of the walls receive the highest amount of reflections and emissions from the opposite wall and from the ground because of the highest view factors. Measurements confirm this behavior on the south wall, where, apart from the underestimate at the highest measurement point, the agreement between simulations and observations looks very good. On the other hand, on the north wall observations show an opposite behavior, with the highest temperatures near the roof. As a consequence, the model overestimates the temperature at the two lowest measurement points in the morning and in the first part of the afternoon.

b. *Air temperatures*

Model results and observations for five consecutive days of the summer field campaign are compared in Fig. 13, along with wind speed measured at Molino Vittoria. Different weather conditions occurred during these days: day 9 August was rainy; days 10, 11, and 13 August were partly cloudy; while day 12 August was sunny. At a first glance the model generally simulates very well the air temperature inside the urban canyon over the whole period even under changing weather conditions. Few overestimates are registered in connection with low wind speeds, which make the simulated heat exchange between the canyon and the atmosphere too low. Indeed, the latter is proportional to the wind velocity: see Eq. (23) in Kusaka et al. (2001). Nevertheless, on all the summer field measurements, the MAE of the model is only 0.4°C. The model simulates slightly better minima than maxima, with MAEs of 0.4° and 0.5°C, respectively. The scatterplot of the measured and simulated temperatures during the whole summer measurements is presented in Fig. 14. The agreement between measured and simulated temperatures appears very satisfactory for all the available data: discrepancies are mostly within 0.5°C and the maximum errors are few overestimates of order 2°C.

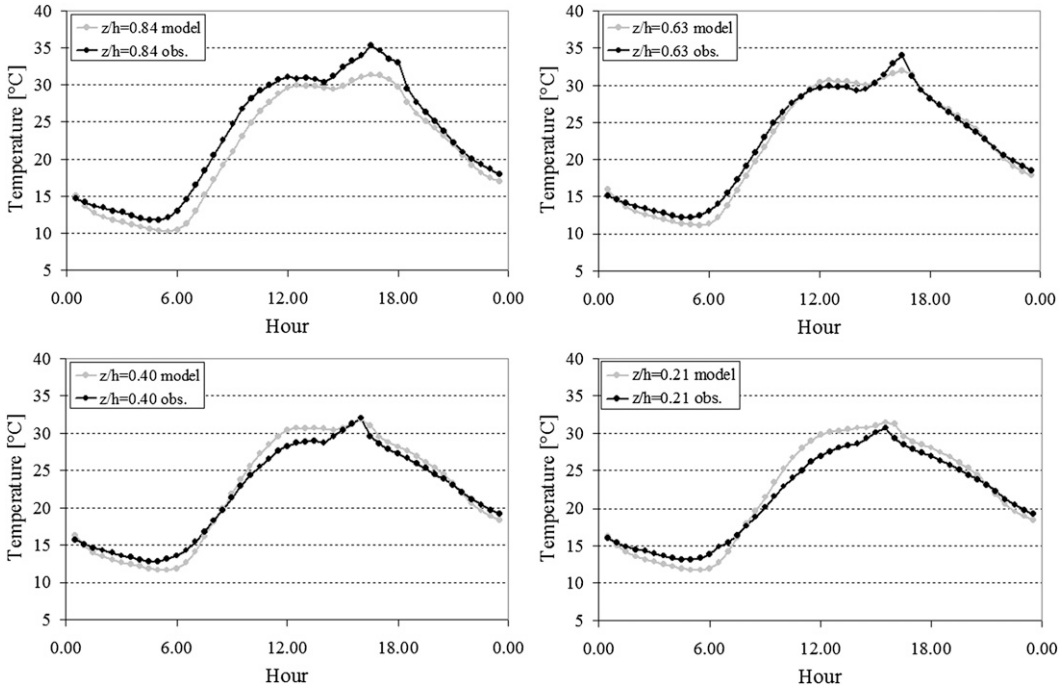

FIG. 12. As in Fig. 11, but for the north wall.

The comparison between the model results and the measurements during five consecutive days of the winter field campaign is shown in Fig. 15. Again days with different weather conditions have been chosen: days 6, 7, and 8 January were cloudy or rainy–snowy; while days 9 and 10 January were sunny. It can be seen that the model is able to simulate with a good accuracy, even better than during the summer period, the average temperature inside the urban canyon. In fact the MAE of the model during the whole winter field campaign is 0.3°C. Even in this case minima are simulated slightly better than maxima, with MAEs of 0.3° and 0.4°C, respectively. The good performance of the model during the whole winter campaign is confirmed again by the scatterplot in Fig. 16, where all the measured and simulated temperatures are compared. It can be seen that the model tends to slightly underestimate low temperatures, as can be partly observed also in Fig. 15. The greatest errors are few overestimates of order 1.5°C, again under low wind speed conditions.

c. Surface energy balance

Apart from direct comparison of measured and simulated air and wall temperatures, it is interesting to inspect how the model simulates the daily cycles of the heat fluxes. Although no data for these variables are available from the present datasets, yet some comparisons can be made with similar literature cases. The results presented in this section refer to the real canyon test case, and the surface fluxes are calculated as they arise from an area having the geometrical characteristics of Via Rosmini. The average daily cycle of the surface energy budget during the sunny days of the summer field measurements is shown in Fig. 17a. The conduction heat flux is the dominant component of the surface energy budget, as found in different field measurements in dense urban areas (e.g., Oke et al. 1999 in Mexico City). Another feature typical of urban areas, and well captured

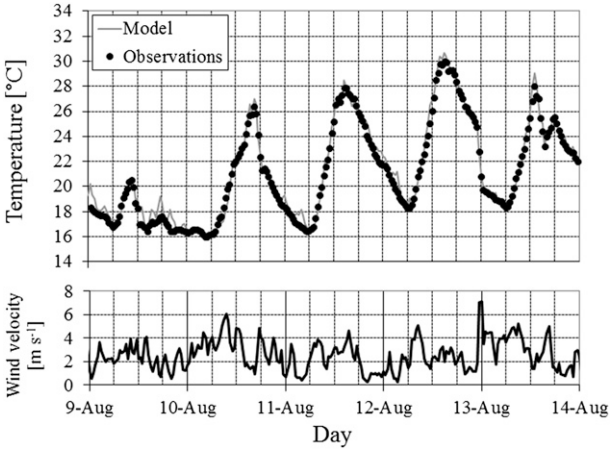

FIG. 13. (top) Comparison (30-min averages) between temperatures measured inside the canyon (black dots) and simulated by the model (gray line) during five consecutive days of the summer field campaign, along with (bottom) wind velocity recorded at Molino Vittoria.

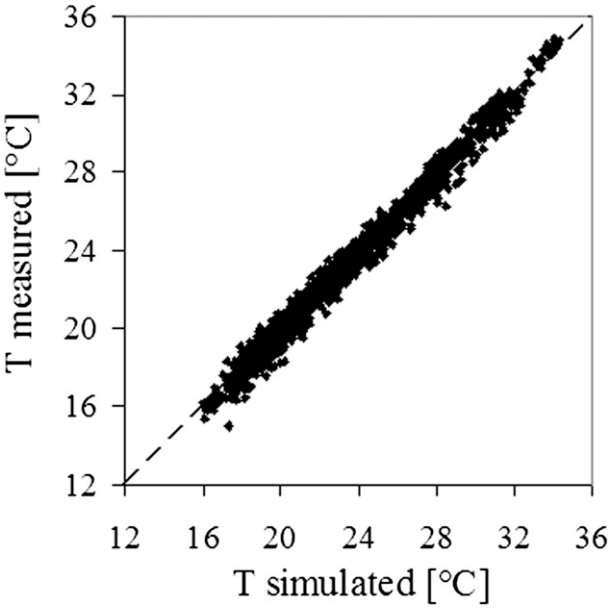

FIG. 14. Scatterplot of measured and simulated average air temperature (30-min averages) inside Via Rosmini for the summer field campaign.

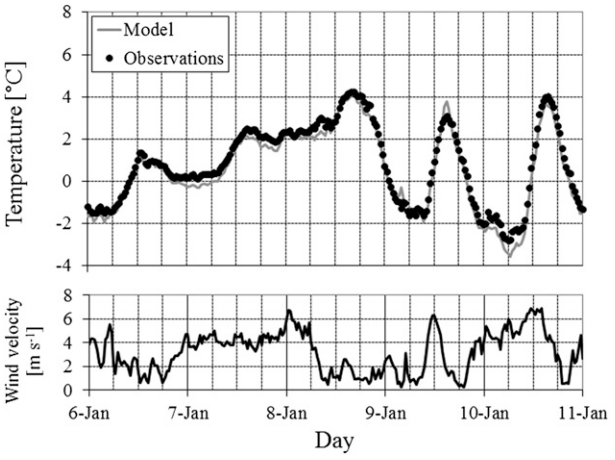

FIG. 15. As in Fig. 13, but for five consecutive days of the winter field campaign.

by the model, is the asymmetry of the peaks in the conduction and sensible heat fluxes: the former peaks around noon, while the latter in the early afternoon (e.g., Coutts et al. 2007). Furthermore, the sensible heat flux remains positive even during nighttime, supported by the heat released by the surfaces. The results for the sunny days of the winter field measurements are presented in Fig. 17b. In this case in the central part of the day the sensible and the conduction heat fluxes display comparable values, and the asymmetry in their peaks is not present. Furthermore, similarly to what observed and simulated with the TEB single-layer model during the winter period by Pigeon et al. (2008) in Marseille, during nighttime the sensible heat flux presents higher values than in the summer period, probably caused by releases from space heating.

5. Summary and discussion

The findings shown in the previous sections can be summarized into some main facts. Field measurements confirmed that the microclimatic conditions inside a typical urban canyon are primarily influenced by the penetration of direct solar radiation inside the canopy and the consequent surface heating. In fact during sunny days the highest temperatures are measured by the east-facing sensors in the morning but in the afternoon by the west-facing ones. Only in the winter period is the overheating of the east-facing sensors in the morning very low, as the wall is hit by the sun for a short time and the morning solar radiation in this period is very weak. The temperature in the center of the street, not influenced by any surface, is always similar to that registered by the sensors in the shade. This suggests that the temperature field inside the urban canyon is quite homogeneous horizontally, with stronger gradients only near the sunlit surfaces. As to the vertical temperature gradients, measurements show that during daytime in the summer period the HOBO at a lower height records slightly higher temperatures than the other instrument on the same wall. For this reason it can be supposed that maxima inside the canyon are reached near ground level in summer, as pointed out by Kanda et al. (2005), probably because of the warming from the road asphalt, which can reach temperatures as high as 50°–60°C during hot summer days (cf. Niachou et al. 2008). Measurements suggest that the temperature field inside the canyon is rather homogeneous in the absence of solar radiation; that is, during the night or in cloudy or rainy days: indeed, temperatures registered by all the sensors are similar.

The temperature inside the canyon is generally higher than above roof level, both in summer and in winter. Higher differences are found during the summer period, also in this case probably because of the stronger overheating of the walls and of the road. Similar results were found by Offerle et al. (2007) in an urban canyon in Gothenburg, Sweden.

As to the validation of the single-layer urban-canyon model, results suggest that this simple scheme can simulate with good accuracy both wall and air temperatures inside the canopy layer, despite the low complexity of the numerical code and the simplifying assumptions. However, some weaknesses have been detected in the simulation of both air and wall temperatures. In particular

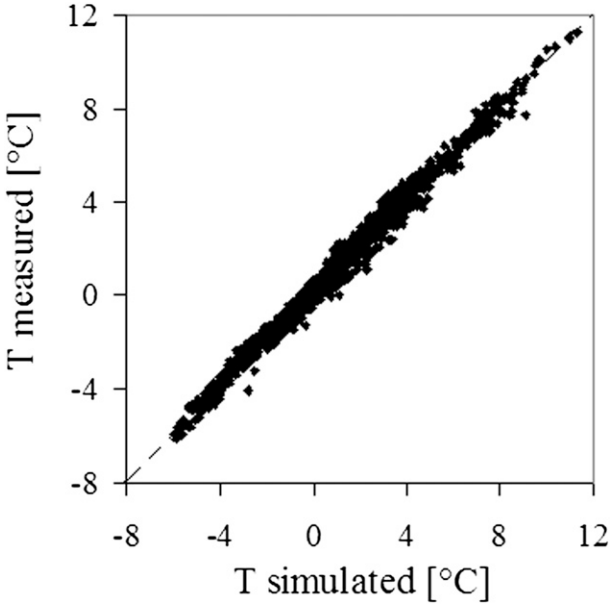

FIG. 16. As in Fig. 14, but for the winter field campaign.

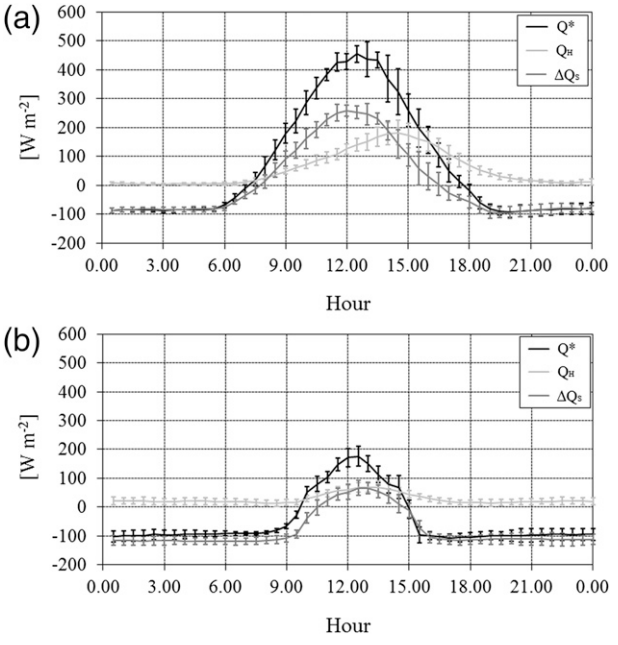

FIG. 17. Average daily cycles of the surface fluxes calculated by the model during the sunny days of the (a) summer and (b) winter field measurements. The Q^* represents the net radiation, Q_H is the sensible heat flux, and ΔQ_S is the conduction heat flux. The vertical bars indicate the standard deviation.

the model tends to overestimate the air temperature under low wind speed conditions. This probably depends on the parameterization of the heat exchange between the canyon air and the atmosphere above roof level, which is proportional to the wind velocity. As to the wall temperature, the model constantly underestimates it in the highest part of both walls. Moreover, the simulation of the north wall temperatures displays some discrepancies from measured values. According to the observations, the temperature of the wall increases from ground level up to the top, while the model shows an opposite behavior. Indeed, in the model the lower parts of the wall receive a greater amount of the radiation emitted and reflected from the opposite wall and from the ground because of the high view factors. The above discrepancies might be caused by local effects not incorporated in the model; for example, the heating of the steel roof might play a role in the underestimate in the highest part of the walls. Other possible causes might be an imperfect characterization of the reflections inside the canyon or an overestimate of the ground temperature. In any case it should be noticed that the accuracy of the results obtained with the simple urban-canyon model is comparable to that obtained with the more complicated 3D finite-elements model utilized in Idczak et al. (2010). In particular, also in Idczak et al. (2010) the temperature was underestimated at the top of both walls and overestimated at the lowest measurement points of the north wall.

The applicability of the canyon model presented here might be extended including effects arising from trees and other vegetation within the street. This issue may be relevant, as vegetation modifies surface energy budgets, promoting latent heat fluxes, and enhances air moisture, which may worsen human comfort conditions. Furthermore, it also affects pollutant dispersion processes (cf. Buccolieri et al. 2009, 2011).

6. Conclusions and outlook on future work

The analyses presented in this paper represent the second step of a project aiming at characterizing the urban climate of the city of Trento. After assessing the main features of the urban heat island at a city scale (Giovannini et al. 2011), the present work focused on a smaller scale, providing some insights on the microclimatic conditions inside the canopy layer. Moreover, the street canyon adopted for the present study displays a geometry and building materials that are rather common in small- to medium-sized European cities, thus allowing us to consider the results as representative for a large number of similar situations.

Giovannini et al. (2011) showed that in Trento the urban heat island intensity, calculated as the temperature difference between the weather station above roof level and measurements collected at rural locations, may reach values up to 5°–6°C during clear nights with low wind speeds. The results of the urban-canyon field

campaigns suggest that the urban heat island inside the canopy layer can be even stronger, with a consequent serious discomfort for the citizens, especially during summer evenings and nights.

As a further step the analysis will be extended to a larger spatial scale, evaluating the influence of the urban area on the local meteorological phenomena typical of an Alpine valley, in particular local circulation systems (cf. Zardi and Whiteman 2013). The latter display peculiar patterns, since they arise as a combination of along-valley and cross-valley flows (cf. Rampanelli et al. 2004) and develop in connection with specific boundary layer properties, as the terrain complexity not only affects the wind regimes and the thermal structure (Rampanelli and Zardi 2004; Rotach and Zardi 2007; Serafin and Zardi 2010a,b, 2011) but also turbulence properties (de Franceschi and Zardi 2003; de Franceschi et al. 2002, 2009) and air quality (de Franceschi and Zardi 2009). To this purpose high-resolution numerical simulations will be performed using a mesoscale meteorological model coupled with parameterization schemes specifically devised for urban areas, such as the model tested in this work.

Acknowledgments. Dr. Jean-Michel Rosant is kindly acknowledged for supplying the data reproduced in Fig. 10 of Idczak et al (2007).

Eng. Daniele Ravanelli provided a valuable technical support during the winter field measurements.

Authors are indebted with colleagues of both the Departments of Economics and Sociology for allowing the installation of the sensors near the walls of the buildings and with Eng. Luca Leonelli (Technologic Networks Office, Municipality of Trento) for installing the sensor on the traffic light.

The Municipality of Trento is also acknowledged for the traffic data contained in the Urban Mobility Plan.

The Italian Center for Meteorology and Climatology of the Italian Air Force and www.wunderground.com provided the data concerning cloud cover at the Mount Paganella weather station.

APPENDIX

Modifications from Kusaka's Model

The model tested in this work is a slightly modified version of the single-layer model by Kusaka et al. (2001). The small modifications are presented in this appendix.

The only radiation measurement input required by the model is the incoming global solar radiation, whereas Kusaka's model needed the direct and diffuse components of the solar radiation and the incoming longwave radiation. In the present model the partitioning of the global solar radiation S_{glob} into direct and diffuse components is calculated according to Carroll (1985). The ratio $\alpha_{\text{diff}} = S_{\text{diff}}/S_{\text{glob}}$, where S_{diff} is the solar diffuse radiation, is calculated as follows:

$$\alpha_{\text{diff}} = 0.88 - 1.024K_t, \tag{A1}$$

with

$$K_t = \frac{S_{\text{glob}}}{K_{\text{sun}}\cos\theta_z}, \tag{A2}$$

where K_{sun} is the solar constant and θ_z is the solar zenith angle. The incoming longwave radiation is calculated according to Brutsaert (1975) and Unsworth and Monteith (1975), to take into account the effects of cloud cover. The atmospheric emissivity with clouds $\varepsilon_a(c)$ is calculated with the following expression (Unsworth and Monteith 1975):

$$\varepsilon_a(c) = (1 - 0.84c)\varepsilon_a(0) + 0.84c, \tag{A3}$$

where c is the fraction of sky covered by clouds and ε_a is the atmospheric emissivity with completely clear sky (Brutsaert 1975):

$$\varepsilon_a(0) = 1.24\left(\frac{e_a}{T_a}\right)^{1/7}, \tag{A4}$$

where e_a (hPa) and T_a (K) are the vapor pressure and the air temperature at the reference station. Finally, the incoming longwave radiation L is calculated from the Stefan–Boltzmann relationship:

$$L = \varepsilon_a(c)\sigma T_a^4, \tag{A5}$$

where σ is the Stefan–Boltzmann constant.

The net amount of short- and longwave radiation absorbed by the surfaces is treated as in Kusaka et al. (2001), taking into account the multiple reflections inside the canyon, but in the present implementation the walls and the road have been divided into different subareas, so that different temperature values can be found in different portions of the same surface. Moreover, the ATREUS–PICADA simulation needed a slight modification in the calculation of the shadowing inside the canyon, to take into account that the physical model is not infinitely long and, as a consequence, solar radiation can reach the walls and the ground also through the canyon ends. Referring to Fig. A1, when solar radiation penetrates inside the canyon through the canyon end, the portion of street in the shade l_{shadow_2} is calculated as

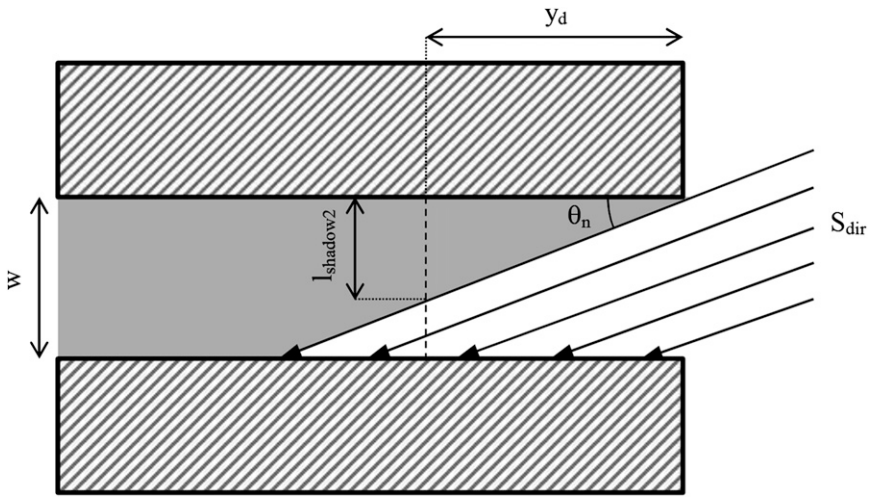

FIG. A1. Plane view of an urban canyon of finite length, along with the solar radiation penetrating inside it from a canyon end. The dashed line represents the cross section considered for the calculation of l_{shadow2}.

$$l_{\text{shadow}_2} = \begin{cases} y_d \tan\theta_n & l_{\text{shadow}_2} < w \\ w & l_{\text{shadow}_2} \geq w \end{cases}, \quad \text{(A6)}$$

where y_d is the distance of the cross section analyzed from the canyon end, and $\theta_n = \theta_{\text{sun}} - \theta_{\text{can}}$, where θ_{sun} is the solar azimuth angle and θ_{can} is the canyon orientation. Then the actual portion of street in shadow l_{shadow} is calculated as follows:

$$l_{\text{shadow}} = \min(l_{\text{shadow}_1}, l_{\text{shadow}_2}), \quad \text{(A7)}$$

where l_{shadow_1} is the portion of street in the shade as calculated in Kusaka et al. (2001):

$$l_{\text{shadow}_1} = \begin{cases} h \tan\theta_z \sin\theta_n & l_{\text{shadow}_1} < w \\ w & l_{\text{shadow}_1} \geq w \end{cases}. \quad \text{(A8)}$$

The heat through the surfaces is calculated, as in Kusaka's model, with the heat conduction equation dividing each surface in several layers, but, as in Masson et al. (2002), an additional resistance to heat transfer ($R_{\text{int}} = 0.123$ m^2 K W^{-1}) has been added at the internal walls and roof layers, to take into account convection and radiation inside the building.

Differently from Kusaka et al. (2001), the temperature of the surface layers is calculated with a prognostic equation, similar to Masson (2000). Thus the following equation is applied at the first layer of the generic ith surface, as highlighted by the subscripts, that is, that directly in contact with the external air:

$$C_{i,1}\frac{\partial T_{i,1}}{\partial t} = \frac{1}{d_{l_{i,1}}}(S_i^* + L_i^* - Q_{H_i} - \Delta Q_{s_{i,1-2}}), \quad \text{(A9)}$$

where C is the heat capacity; T is the temperature of the layer; d_l is the thickness of the layer; S^* and L^* are the net short- and longwave radiations, respectively; Q_H is the sensible heat flux, and ΔQ_s is the conduction heat flux between layers 1 and 2. From Eq. (A9) it can be seen that in the model tested here, as said in section 3a, the latent heat flux is not considered.

The anthropogenic heat flux from vehicular traffic Q_v is calculated by means of Grimmond's (1992) formula:

$$Q_v = \frac{n_v D_v \text{EV}}{A \times 3600} \ (\text{W m}^{-2}), \quad \text{(A10)}$$

where

$$\text{EV} = \text{NHC}\rho_f/\text{FE} \ (\text{J m}^{-1}),$$

n_v are the hourly vehicular fluxes, D_v (m) is the length of the road, A (m^2) is the area considered, NHC (J kg^{-1}) is the net heat of combustion, ρ_f (kg L^{-1}) is the density of fuel, and FE (m L^{-1}) is the mean fuel economy. The values of NHC, ρ_f, and FE adopted in the present study have been chosen from typical values present in the literature (NHC = 45×10^6 J kg^{-1}, $\rho_f = 0.75$ kg L^{-1}, and FE = 8500 m L^{-1}; Sailor and Lu 2004).

REFERENCES

Bertò, A., A. Buzzi, and D. Zardi, 2004: Back-tracking water vapour contributing to a precipitation event over Trentino: A case study. *Meteor. Z.,* **13,** 189–200.

Bourbia, F., and H. B. Awbi, 2004: Building cluster and shading in urban canyon for hot dry climate. Part I: Air and surface temperature measurements. *Renewable Energy,* **29,** 249–262.

Brutsaert, W., 1975: On a derivable formula for long-wave radiation from clear skies. *Water Resour. Res.,* **11,** 742–744.

Buccolieri, R., C. Gromke, S. Di Sabatino, and B. Ruck, 2009: Aerodynamic effects of trees on pollutant concentration in street canyons. *Sci. Total Environ.,* **407,** 5247–5256.

——, S. M. Salim, L. S. Leo, S. Di Sabatino, A. Chan, P. Ielpo, G. de Gennaro, and C. Gromke, 2011: Analysis of local scale tree-atmosphere interaction on pollutant concentration in idealized street canyons and application to a real urban junction. *Atmos. Environ.,* **45,** 1702–1713.

Carroll, J. J., 1985: Global transmissivity and diffuse fraction of solar radiation for clear and cloudy skies as measured and as predicted by bulk transmissivity models. *Sol. Energy,* **2,** 105–118.

Chen, F., and Coauthors, 2011: The integrated WRF/urban modeling system: Development, evaluation, and applications to urban environment problems. *Int. J. Climatol.,* **31,** 273–288.

Coutts, A. M., J. Beringer, and N. J. Tapper, 2007: Impact of increasing urban density on local climate: Spatial and temporal variations in the surface energy balance in Melbourne, Australia. *J. Appl. Meteor. Climatol.,* **46,** 477–493.

de Franceschi, M., and D. Zardi, 2003: Evaluation of cut-off frequency and correction of filter-induced phase lag and attenuation in eddy covariance analysis of turbulence data. *Bound.-Layer Meteor.,* **108,** 289–303.

——, and ——, 2009: Study of wintertime high pollution episodes during the Brenner-South ALPNAP measurement campaign. *Meteor. Atmos. Phys.,* **103,** 237–250.

——, G. Rampanelli, and D. Zardi, 2002: Further investigations of the ''Ora del Garda'' valley wind. Preprints, *10th Conf. on Mountain Meteorology*, Park City, UT, Amer. Meteor. Soc., 3.2. [Available online at http://ams.confex.com/ams/pdfpapers/39949.pdf.]

——, D. Zardi, M. Tagliazucca, and F. Tampieri, 2009: Analysis of second order moments in the surface layer turbulence in an Alpine valley. *Quart. J. Roy. Meteor. Soc.,* **135,** 1750–1765.

de Munck, C., and Coauthors, 2013: How much can air conditioning increase air temperatures for a city like Paris, France? *Int. J. Climatol.,* doi:10.1002/joc.3415, in press.

Doran, J. C., C. M. Berkowitz, R. L. Coulter, W. J. Shaw, and C. W. Spicer, 2003: The 2001 Phoenix Sunrise experiment: Vertical mixing and chemistry during the morning transition in Phoenix. *Atmos. Environ.,* **37,** 2365–2377.

Erell, E., and T. Williamson, 2007: Intra-urban differences in canopy layer air temperature at a mid-latitude city. *Int. J. Climatol.,* **27,** 1243–1255.

Fast, J. D., J. C. Torcolini, and D. Redman, 2005: Pseudovertical temperature profiles and the urban heat island measured by a temperature datalogger network in Phoenix, Arizona. *J. Appl. Meteor.,* **44,** 2–13.

Georgakis, C., and M. Santamouris, 2006: Experimental investigation of air flow and temperature distribution in deep urban canyons for natural ventilation purposes. *Energy Build.,* **38,** 367–376.

Giovannini, L., D. Zardi, and M. de Franceschi, 2011: Analysis of the urban thermal fingerprint of the city of Trento in the Alps. *J. Appl. Meteor. Climatol.,* **50,** 1145–1162.

Grigiante, M., F. Mottes, D. Zardi, and M. de Franceschi, 2011: Experimental solar radiation measurements and their effectiveness in setting up a real sky irradiance model. *Renewable Energy,* **36,** 1–8.

Grimmond, C. S. B., 1992: The suburban energy balance: Methodological considerations and results for a mid-latitude west coast city under winter and spring conditions. *Int. J. Climatol.,* **12,** 481–497.

——, 2006: Progress in measuring and observing the urban atmosphere. *Theor. Appl. Climatol.,* **84,** 3–22.

——, and T. R. Oke, 1999: Aerodynamic properties of urban areas derived from analysis of surface form. *J. Appl. Meteor.,* **38,** 1262–1292.

——, M. Best, and J. Barlow, 2008: Urban surface energy balance models: Model characteristics and methodology for a comparison study. *Urbanization of Meteorological and Air Quality Models,* A. Baklanov et al., Eds., Springer, 76–97.

——, and Coauthors, 2010: The international urban energy balance models comparison project: First results from phase 1. *J. Appl. Meteor. Climatol.,* **49,** 1268–1292.

——, and Coauthors, 2011: Initial results from phase 2 of the international urban energy balance model comparison. *Int. J. Climatol.,* **31,** 244–272.

Hamdi, R., and G. Schayes, 2007: Validation of Martilli's urban boundary layer scheme with measurements from two mid-latitude European cities. *Atmos. Chem. Phys.,* **7,** 4513–4526.

——, and V. Masson, 2008: Inclusion of a drag approach in the Town Energy Balance (TEB) scheme: Offline 1D evaluation in a street canyon. *J. Appl. Meteor. Climatol.,* **47,** 2627–2644.

——, and G. Schayes, 2008: Sensitivity study of the urban heat island intensity to urban characteristics. *Int. J. Climatol.,* **28,** 973–982.

Idczak, M., P. Mestayer, J.-M. Rosant, J.-F. Sini, and M. Violleau, 2007: Micrometeorological measurements in a street canyon during the joint ATREUS-PICADA experiment. *Bound.-Layer Meteor.,* **124,** 25–41.

——, D. Groleau, P. Mestayer, J.-M. Rosant, and J.-F. Sini, 2010: An application of the thermo-radiative model SOLENE for the evaluation of street canyon energy balance. *Build. Environ.,* **45,** 1262–1275.

Kanda, M., R. Moriwaki, and Y. Kimoto, 2005: Temperature profiles within and above an urban canopy. *Bound.-Layer Meteor.,* **115,** 499–506.

Kusaka, H., H. Kondo, Y. Kinegawa, and F. Kimura, 2001: A simple single-layer urban canopy model for atmospheric models: Comparison with multi-layer and slab models. *Bound.-Layer Meteor.,* **101,** 329–358.

Lemonsu, A., and V. Masson, 2002: Simulation of a summer urban breeze over Paris. *Bound.-Layer Meteor.,* **104,** 463–490.

——, C. S. B. Grimmond, and V. Masson, 2004: Modeling the surface energy balance of the core of an old Mediterranean city: Marseille. *J. Appl. Meteor.,* **43,** 312–327.

Martilli, A., A. Clappier, and M. W. Rotach, 2002: An urban surface exchange parameterization for mesoscale models. *Bound.-Layer Meteor.,* **104,** 261–304.

Masson, V., 2000: A physically-based scheme for the urban energy budget in atmospheric models. *Bound.-Layer Meteor.,* **94,** 357–397.

——, 2006: Urban surface modeling and the meso-scale impact of cities. *Theor. Appl. Climatol.,* **84,** 35–45.

——, C. S. B. Grimmond, and T. R. Oke, 2002: Evaluation of the town energy balance (TEB) scheme with direct measurements from dry districts in two cities. *J. Appl. Meteor.,* **41,** 1011–1026.

Mestayer, P. G., and Coauthors, 2005: The urban boundary layer field campaign in Marseille (UBL/CLU-ESCOMPTE): Set-up and first results. *Bound.-Layer Meteor.,* **114,** 315–365.

Municipality of Trento, cited 2009: Trento statistica, la popolazione al 31 dicembre 2008 (Statistical Trento, population at

31 December 2008). [Available online at http://www3.comune.trento.it/content/download/291215/2787510/file/trento_statistica_2008.pdf.]

Niachou, K., I. Livada, and M. Santamouris, 2008: Experimental study of temperature and airflow distribution inside an urban street canyon during hot summer weather conditions—Part I: Air and surface temperatures. *Build. Environ.,* **43,** 1383–1392.

Offerle, B., I. Eliasson, C. S. B. Grimmond, and B. Holmer, 2007: Surface heating in relation to air temperature, wind and turbulence in an urban street canyon. *Bound.-Layer Meteor.,* **122,** 273–292.

Ohashi, Y., Y. Genchi, H. Kondo, Y. Kikegawa, H. Yoshikado, and Y. Hirano, 2007: Influence of air-conditioning waste heat on air temperature in Tokyo during summer: Numerical experiments using an urban canopy model coupled with a building energy model. *J. Appl. Meteor. Climatol.,* **46,** 66–81.

Oke, T. R., 1976: The distinction between canopy and boundary layer urban heat islands. *Atmosphere,* **14,** 268–277.

——, 1981: Canyon geometry and the nocturnal heat island. Comparison of scale model and field observations. *J. Climatol.,* **1,** 237–254.

——, 2006: Initial guidance to obtain representative meteorological observations at urban sites. WMO/TD 1250, 47 pp.

——, R. A. Spronken-Smith, E. Jáuregui, and C. S. B. Grimmond, 1999: The energy balance of central Mexico City during the dry season. *Atmos. Environ.,* **33,** 3919–3930.

Pigeon, G., M. A. Moscicki, J. A. Voogt, and V. Masson, 2008: Simulation of fall and winter surface energy balance over a dense urban area using the TEB scheme. *Meteor. Atmos. Phys.,* **102,** 159–171.

Rampanelli, G., and D. Zardi, 2004: A method to determine the capping inversion of the convective boundary layer. *J. Appl. Meteor.,* **43,** 925–933.

——, ——, and R. Rotunno, 2004: Mechanisms of up-valley winds. *J. Atmos. Sci.,* **61,** 3097–3111.

Rotach, M. W., and D. Zardi, 2007: On the boundary layer structure over highly complex terrain: Key findings from MAP. *Quart. J. Roy. Meteor. Soc.,* **133,** 937–948.

——, and Coauthors, 2005: BUBBLE—An urban boundary layer meteorology project. *Theor. Appl. Climatol.,* **81,** 231–261.

Roulet, Y.-A., A. Martilli, M. W. Rotach, and A. Clappier, 2005: Validation of an urban surface exchange parameterization for mesoscale models-1D case in a street canyon. *J. Appl. Meteor.,* **44,** 1484–1498.

Sailor, D. J., and L. Lu, 2004: A top-down methodology for developing diurnal and seasonal anthropogenic heating profiles for urban areas. *Atmos. Environ.,* **38,** 2737–2748.

Santamouris, M., N. Papanikolaou, I. Koronakis, I. Livada, and D. Asimakopoulos, 1999: Thermal and air flow characteristics in a deep pedestrian canyon under hot weather conditions. *Atmos. Environ.,* **33,** 4503–4521.

Serafin, S., and D. Zardi, 2010a: Structure of the atmospheric boundary layer in the vicinity of a developing upslope flow system: A numerical model study. *J. Atmos. Sci.,* **67,** 1171–1185.

——, and ——, 2010b: Daytime heat transfer processes related to slope flows and turbulent convection in an idealized mountain valley. *J. Atmos. Sci.,* **67,** 3739–3756.

——, and ——, 2011: Daytime development of the boundary layer over a plain and in a valley under fair weather conditions: A comparison by means of idealized numerical simulations. *J. Atmos. Sci.,* **68,** 2128–2141.

Shepherd, J. M., 2005: A review of current investigations of urban-induced rainfall and recommendations for the future. *Earth Interact.,* **9,** 1–27. [Available online at http://EarthInteractions.org.]

Svensson, M. K., 2004: Sky view factor analysis—Implications for urban air temperature differences. *Meteor. Appl.,* **11,** 201–211.

Unsworth, M. H., and J. L. Monteith, 1975: Long-wave radiation at the ground. *Quart. J. Roy. Meteor. Soc.,* **101,** 13–24.

Whiteman, C. D., J. M. Hubbe, and W. J. Shaw, 2000: Evaluation of an inexpensive temperature datalogger for meteorological applications. *J. Atmos. Oceanic Technol.,* **17,** 76–81.

Zardi, D., and C. D. Whiteman, 2013: Diurnal mountain wind systems. *Mountain Weather Research and Forecasting: Recent Progress and Current Challenges,* F. K. Chow, S. F. J. De Wekker, and B. Snyder, Eds., Springer, 35–119.